# NOTES AND CORRESPONDENCE

## On the Transport and Angular Momentum Balance of Channel Models of the Antarctic Circumpolar Current

DAVID N. STRAUB

*University of Washington, School of Oceanography, Seattle, Washington*

19 November 1991, 27 April 1992

ABSTRACT

Angular momentum balances are discussed, both in general as well as in the context of simple channel models of the Antarctic Circumpolar Current (ACC). Particular emphasis is placed on the close relationship between the angular momentum balance and the meridional circulation. It is found that topographic form drag is established very early in the integration, whereas interfacial form drag can take much longer to develop.

Restrictions on the geostrophic portion of the meridional circulation imposed by zonally reconnecting potential vorticity contours in the upper ocean allow derivation of an estimate for the steady-state transport. The estimate assumes there to be little or no circumpolar flow at great depth, an assumption that stems from the belief that the band of zonally reconnecting geostrophic contours in the Southern Ocean does not extend to the ocean floor. The predicted transport is proportional to the strength of the stratification and compares favorably with numerical results in the literature. Interaction of the ACC with the two adjoining gyres, however, is not accounted for by this estimate. The implications of this for the total transport through Drake Passage are discussed.

### 1. Introduction

In this paper, we revisit the dynamics of wind-driven flow in a channel from an angular momentum perspective, paying particular attention to the relationship between angular momentum and the meridional circulation. Globally, angular momentum is imparted to the Southern Ocean by the winds and is removed primarily by topographic form stresses between the ocean and the solid earth (Munk and Palmeń 1951). Similarly, the vertical transfer of angular momentum through the water column is believed to be accomplished primarily by interfacial form stresses between, say, the various layers of a multilayered model. This scenario was confirmed numerically in the context of an eddy-resolving quasigeostrophic model by McWilliams et al. (1978). More recently, Treguier and McWilliams (1990, hereafter TM) and Wolff et al. (1991, hereafter WMRO) have addressed the relative roles of standing and transient eddies and have begun to explore the parameter space of possible topographies.

Perhaps the simplest explanation of the strength of the Antarctic Circumpolar Current (ACC) is the suggestion (e.g., Stommel 1957) that a southward Sverdrup transport into the Southern Ocean accounts for the transport through Drake Passage. By this view the ACC is seen as a poleward boundary current for the thin subpolar gyre lying to its north. Baker (1982) estimates the implied circumpolar transport to be 161 $\pm$ 69 Sv (Sv $\equiv 10^6$ m$^3$ s$^{-1}$), which is in reasonable agreement with observations. This view of the ACC does not, however, explain the dynamics of that part of the Southern Ocean containing zonally reconnecting potential vorticity contours, where we do not expect Sverdrup dynamics to apply. Here, we view the total ACC transport to be the sum of two components: one due to interaction with the subpolar gyre and another due to the dynamics of the channellike portion of the Southern Ocean alone. Baker's estimate of transport then corresponds to the former of these. Given the magnitude of his estimate, we expect that the latter of the two components should be small or slightly negative (e.g., westward).

In section 2, we define "relative" and "planetary" angular momentum and discuss the relationship between angular momentum balances and meridional circulation. In section 3, we consider the angular momentum balance during the spinup phase of a two-layer channel model. Topography takes the form of a meridional ridge sufficiently high so that there are no free contours of potential vorticity in the lower layer. This choice is motivated by the belief that the abyssal portion of the Southern Ocean is not channellike, but contains large topographic features that tend to prohibit circumpolar flow in the abyssal layers. We find that, unlike

*Corresponding author address:* Dr. David N. Straub, NERC Ocean Unit, Department of Atmospheric, Oceanic and Planetary Physics, Clarendon Laboratory, Parks Rd., Oxford OX1 3PO, United Kingdom.

# NOTES AND CORRESPONDENCE

## On the Transport and Angular Momentum Balance of Channel Models of the Antarctic Circumpolar Current

DAVID N. STRAUB

*University of Washington, School of Oceanography, Seattle, Washington*

19 November 1991, 27 April 1992

ABSTRACT

Angular momentum balances are discussed, both in general as well as in the context of simple channel models of the Antarctic Circumpolar Current (ACC). Particular emphasis is placed on the close relationship between the angular momentum balance and the meridional circulation. It is found that topographic form drag is established very early in the integration, whereas interfacial form drag can take much longer to develop.

Restrictions on the geostrophic portion of the meridional circulation imposed by zonally reconnecting potential vorticity contours in the upper ocean allow derivation of an estimate for the steady-state transport. The estimate assumes there to be little or no circumpolar flow at great depth, an assumption that stems from the belief that the band of zonally reconnecting geostrophic contours in the Southern Ocean does not extend to the ocean floor. The predicted transport is proportional to the strength of the stratification and compares favorably with numerical results in the literature. Interaction of the ACC with the two adjoining gyres, however, is not accounted for by this estimate. The implications of this for the total transport through Drake Passage are discussed.

### 1. Introduction

In this paper, we revisit the dynamics of wind-driven flow in a channel from an angular momentum perspective, paying particular attention to the relationship between angular momentum and the meridional circulation. Globally, angular momentum is imparted to the Southern Ocean by the winds and is removed primarily by topographic form stresses between the ocean and the solid earth (Munk and Palmeń 1951). Similarly, the vertical transfer of angular momentum through the water column is believed to be accomplished primarily by interfacial form stresses between, say, the various layers of a multilayered model. This scenario was confirmed numerically in the context of an eddy-resolving quasigeostrophic model by McWilliams et al. (1978). More recently, Treguier and McWilliams (1990, hereafter TM) and Wolff et al. (1991, hereafter WMRO) have addressed the relative roles of standing and transient eddies and have begun to explore the parameter space of possible topographies.

Perhaps the simplest explanation of the strength of the Antarctic Circumpolar Current (ACC) is the suggestion (e.g., Stommel 1957) that a southward Sverdrup transport into the Southern Ocean accounts for the transport through Drake Passage. By this view the ACC is seen as a poleward boundary current for the thin subpolar gyre lying to its north. Baker (1982) estimates the implied circumpolar transport to be 161 ± 69 Sv (Sv ≡ $10^6$ $m^3$ $s^{-1}$), which is in reasonable agreement with observations. This view of the ACC does not, however, explain the dynamics of that part of the Southern Ocean containing zonally reconnecting potential vorticity contours, where we do not expect Sverdrup dynamics to apply. Here, we view the total ACC transport to be the sum of two components: one due to interaction with the subpolar gyre and another due to the dynamics of the channellike portion of the Southern Ocean alone. Baker's estimate of transport then corresponds to the former of these. Given the magnitude of his estimate, we expect that the latter of the two components should be small or slightly negative (e.g., westward).

In section 2, we define "relative" and "planetary" angular momentum and discuss the relationship between angular momentum balances and meridional circulation. In section 3, we consider the angular momentum balance during the spinup phase of a two-layer channel model. Topography takes the form of a meridional ridge sufficiently high so that there are no free contours of potential vorticity in the lower layer. This choice is motivated by the belief that the abyssal portion of the Southern Ocean is not channellike, but contains large topographic features that tend to prohibit circumpolar flow in the abyssal layers. We find that, unlike

*Corresponding author address:* Dr. David N. Straub, NERC Ocean Unit, Department of Atmospheric, Oceanic and Planetary Physics, Clarendon Laboratory, Parks Rd., Oxford OX1 3PO, United Kingdom.

topographic form drag, which is established rather quickly, interfacial form stresses can take much longer to develop. Section 4 then uses restrictions imposed on the meridional circulation by the channellike nature of the upper layer to argue that transient eddies are necessary to close the meridional circulation. This is in agreement with TM, who show that transient eddies are needed to balance the energy budget in a statistically steady state. This necessity for eddies (and by implication for baroclinic instability) in the statistically steady state is then used to derive an estimate for the transport of the channellike portion of the Southern Ocean. This estimate, applicable to a wide class of topographies, is sufficiently small so that, when combined with Baker's estimate (for that part of the transport related to interactions with the subpolar gyre), plausible values for the total transport are obtained.

## 2. Relative and planetary angular momentum

We start by defining the angular momentum density of a water parcel as

$$\mathbf{L} = \mathbf{r} \times \rho \mathbf{U}_{\text{total}}, \qquad (2.1)$$

where $\mathbf{r}$ is the position vector with respect to the center of the earth and $\rho \mathbf{U}_{\text{total}}$ specifies the total linear momentum density. For motions whose time scales are long compared to the rotational period, time averaging eliminates all terms excepting those parallel to the earth's axis. In this limit, therefore, the relevant angular momentum is that about the earth's rotational axis. That is,

$$L = \rho R \cos\theta (\Omega R \cos\theta + u), \qquad (2.2)$$

where $\Omega$ is the earth's angular velocity, $u$ is the eastward component of the parcel's velocity (measured in the rotating frame), and $R \cos\theta$ is the distance to the earth's rotational axis, expressed as a function of latitude $\theta$. Expanding the bracket on the rhs of (2.2), we obtain two terms. The first corresponds to the angular momentum associated with the solid body rotation of the earth and the second corresponds to the angular momentum associated with motions relative to the rotating frame of reference. We will refer to the former as the planetary component $L_P$, and to the latter as the relative component $L_R$:

$$L_P \equiv \rho \Omega R^2 \cos^2\theta, \qquad (2.3a)$$

$$L_R \equiv \rho R u \cos\theta. \qquad (2.3b)$$

It is interesting to review some basic balances from an angular momentum perspective. To this end, consider the material derivative of $L_P$:

$$\frac{DL_P}{Dt} = (v/R) \frac{\partial L_P}{\partial \theta} = -fvR \cos\theta, \qquad (2.4)$$

where $v$ is the northward velocity component, $f$ is the Coriolis frequency, and $\rho$ is assumed constant (and taken to be unity). If we substitute the geostrophic approximation for $v$ into (2.4), we obtain

$$(v_{\text{geostrophic}}/R) \frac{\partial L_P}{\partial \theta} = R \cos\theta \frac{-P_\lambda}{R \cos\theta} = -P_\lambda, \qquad (2.5)$$

where $-P_\lambda$ is the pressure torque per unit volume (i.e., $\lambda$ denotes longitude). Thus, at latitudes where geostrophic scaling remains valid, large-scale pressure torques may be interpreted as resulting in a meridional advection of mass by the geostrophic velocity field. A positive torque on a water parcel, for example, causes that parcel to increase its planetary angular momentum as it is advected towards the equator by the geostrophic velocity field.

The relationship between Ekman transport and wind-stress torques is similar. That is, the net change in $L_P$ associated with meridional advection by the Ekman velocity field is balanced by the wind torque (equivalently, by the vertical integral of $R \cos\theta (\nu u_z)_z$ over the Ekman layer). From Ekman theory, the meridional transport associated with the Ekman layer, $V_E$, is given by $V_E = -\tau^x/f$. The associated change in $L_P$ is thus

$$\frac{V_E}{R} \frac{\partial L_P}{\partial \theta} = \frac{\tau^x}{f} (fR \cos\theta) = \tau^x R \cos\theta, \qquad (2.6)$$

where the term on the far rhs is the wind-stress torque. Thus, we can think of positive wind torques as resulting in an advection of water to higher values of $L_P$, this time by the Ekman velocity field. A similar balance can also be found for bottom and internal Ekman layers by replacing $\tau^x$ by the relevant frictional stresses.

The remaining terms in the angular momentum balance of a water parcel include changes in relative angular momentum, advection of planetary angular momentum by the interior ageostrophic portion of the velocity field (i.e., that part of the ageostrophic velocity field not associated with the vertical diffusion of momentum in the Ekman layer), and frictional torques. We thus have

$$\frac{DL_R}{Dt} + \frac{v_a}{R} \frac{\partial L_P}{\partial \theta} = R \cos\theta \nu_h (\nabla^2 \mathbf{u}) \cdot \mathbf{i}, \qquad (2.7)$$

where $\mathbf{i}$ is a unit vector pointing eastward, $v_a$ is the northward component of the interior ageostrophic velocity, and $\nu_h$ is the horizontal eddy viscosity coefficient. Thus, following a parcel of water, changes in $L_R$ are associated with that part of the meridional flow field not balanced by either frictional or pressure torques.

We now consider, more globally, how a perturbation to the rest-state angular momentum in a channel is partitioned between its planetary and relative components. As an illustrative example, consider a single-layer geostrophically balanced zonal flow in a channel bounded by zonal walls at $\theta = \theta_1$ and $\theta = \theta_2$. Take the rest state to be perturbed such that there is a linear gradient in the interface height field $\eta$ across the channel. That is,

$$\eta = a\theta', \tag{2.8}$$

where $\theta' = \theta - \theta_0$, with $\theta_0$ chosen such that there is no net addition of mass to the system. The meridional mass redistribution associated with the tilting of the interface constitutes a perturbation to the average value of $L_P$, while the zonal current implies a change in $L_R$. Let $M_P$ and $M_R$ be the volume integrals over the channel of these two perturbations in $L$. Thus, $M_P$ and $M_R$ represent the total planetary and relative perturbations of angular momentum over the volume in question. We would like to obtain an estimate of the ratio of $M_P$ to $M_R$. The perturbation planetary angular momentum (per radian longitude) in the channel given by

$$M_P = \int_{\theta_1'}^{\theta_2'} aR^2 L_P \theta' \cos(\theta_0 + \theta') d\theta', \tag{2.9}$$

where $\theta_1'$ and $\theta_2'$ are given by $\theta_1 - \theta_0$ and $\theta_2 - \theta_0$, respectively. One could, of course, evaluate the integral in (2.9) exactly, but as we are merely interested in an estimate of the ratio of $M_P$ to $M_R$, we choose to simplify the integral by expanding the integrand in a Taylor series about $\theta_0$. Keeping only the linear term in $\theta'$, we have that

$$M_P \approx a\Omega R^4 \int_{\theta_1'}^{\theta_2'} \theta'(\cos^3\theta_0 - 3\cos^2\theta_0 \sin\theta_0 \theta') d\theta'. \tag{2.10}$$

The requirement that the perturbation not add any net mass to the system implies

$$\int_{\theta_1'}^{\theta_2'} \theta' \cos(\theta_0 + \theta') d\theta' = 0$$

or

$$\int_{\theta_1'}^{\theta_2'} \theta' \cos\theta_0 d\theta' \approx \int_{\theta_1'}^{\theta_2'} (\theta')^2 \sin\theta_0 d\theta'. \tag{2.11}$$

Combining (2.10) and (2.11) then leads to

$$M_P \approx \frac{a(\Delta\theta')^3 (f_0 R^4 \cos^2\theta_0)}{12}, \tag{2.12}$$

where $\Delta\theta' = \theta_2 - \theta_1$ and $f_0$ is $f$, evaluated at $\theta_0$. To the same order of approximation, the relative angular momentum per radian longitude is given by

$$M_R \approx (\text{transport})(R^2 \cos\theta_0) \approx \frac{gaDR^2\Delta\theta' \cos\theta_0}{f_0}, \tag{2.13}$$

where $D$ is the depth of the channel. The ratio of $M_P$ to $M_R$ is then given by

$$\frac{M_P}{M_R} \approx \frac{(f_0 R \Delta\theta')^2}{12gD} = \frac{L_y^2}{12 l_\rho^2}, \tag{2.14}$$

where $L_y = R\Delta\theta'$ is the width of the channel and $l_\rho$ is the (external) Rossby radius.

Thus, assuming the external Rossby radius to be comparable to or larger than the channel width, we see that the vast majority of perturbation angular momentum in the channel is contained by $M_R$. In fact, in the limit of a rigid lid, no net meridional mass redistribution is allowed and $M_P$ is identically zero. In that case, all of the perturbation angular momentum goes to $M_R$. Similarly, in a multilayered, Boussinesq ocean with a rigid lid, there can be no net change in the volume integral of $L_P$. If, for example, water moves poleward in one layer (decreasing $L_P$), an equal amount of water must move equatorward in another layer (increasing $L_P$). Within a single layer of such an ocean, however, the situation is quite different. In fact, for currents with baroclinic structure, most of the net change in the total angular momentum of a single layer is typically accounted for by $M_P$. Consider, for example, the lower layer in a two-layer ocean: Assume that the thermal wind shear between the layers is identical to eastward current in the preceding barotropic calculation and that the net transport vanishes. Then the ratio of $M_P$ to $M_R$ is as before, except that $l_\rho$ is now the baroclinic Rossby radius and $M_P$ and $M_R$ are integrals over the lower layer. Thus, for example, if the (internal) Rossby radius is taken to be 50 km and the channel is taken to be 1000 km wide, then the ratio of $M_P$ to $M_R$ is about $33 \gg 1$. Therefore, while the meridional redistribution of mass plays only a very limited role in the total angular momentum budget of an entire basin, it can play a dominant role in the angular momentum budget of a single layer.

## 3. The angular momentum balance of a two-layer model during spinup

Although the ability to remove angular momentum from the channel is a necessary condition for the establishment of a statistically steady state (of wind-driven flow in a channel), it is not sufficient. In fact, a net topographic form drag nearly equal and opposite to the wind stress typically develops in the first few months of integration. The ultimate statistically steady state, by contrast, typically takes several years to develop. This can be inferred, for example, from the time series of transport shown in WMRO. Their Figs. 9 and 15 show an increase in transport (the quasigeostrophic equivalent $M_R$) over the first five years of integration. This increase is, however, much less than what would be expected assuming little or no removal of angular momentum from the channel. Furthermore, scale analysis shows frictional torques to be small. Therefore, topographic form drag must be removing angular momentum from the system at a rate nearly equal to the rate at which angular momentum is being input by the winds.

In contrast to the quick development of topographic form drag, interfacial form drag can take much longer to develop. To illustrate this, we consider the spinup from rest of wind-driven flow in a two-layer channel model. Topography is assumed to extend across the channel (e.g., a meridional ridge) and to be entirely immersed in the lower layer. Furthermore, the amplitude of the topography is taken to be sufficiently large so as to induce blocked contours of potential vorticity in the lower layer. This choice is motivated by the belief that zonally reconnecting geostrophic contours do not exist in the abyssal Southern Ocean. After just a few inertial periods, an Ekman layer (taken to be embedded in the upper layer) will be established so that the wind-stress torque is balanced by the increase in $L_P$ associated with the equatorward flux in the Ekman layer. A similar amount of angular momentum is being removed from the channel via topographic form drag; therefore, there must be a geostrophic poleward flow, nearly equal and opposite to the Ekman flux, somewhere in the water column.

In the lower layer, where there are no zonally reconnecting potential vorticity contours, such a flow is easily established. In the upper layer, by contrast, such meridional mass fluxes are not so readily established. This is a consequence of the presence of zonally reconnecting geostrophic contours in that layer. It is well known, for example, that the net geostrophic mass flux across a closed geostrophic contour is identically zero. That is,

$$\oint_{q_1=q_0} d(\mathbf{v}_g \cdot \mathbf{n})d\lambda = \oint_{q_1=q_0} d\left(\frac{\partial p/\partial\lambda}{f}\right)d\lambda = \oint_{q_1=q_0} q_0(\partial p/\partial\lambda)d\lambda = 0, \quad (3.1)$$

where $n$ and $\lambda$ are coordinates perpendicular and parallel to the geostrophic contour ($q_1 = q_0$, where $q_1 \equiv d_1/f$), respectively, and $d$, $\mathbf{v}_g$, and $f$ are the upper-layer thickness, geostrophic velocity, and Coriolis frequency, respectively. The subscript 1 refers to the upper layer.

We now use (3.1) to derive an expression for the geostrophic flux across a latitude circle $\theta = \theta_0$, which intersects the zonally reconnecting geostrophic contour. First, define $\Sigma$ to be the "area" enclosed by the geostrophic contour and latitude circle in question, with area south of $\theta = \theta_0$ considered negative and area north of $\theta = \theta_0$ considered positive (see Fig. 1). Let $V$ be the corresponding volume of water in the upper layer. The time derivative of $V$ is then given by

$$\frac{dV}{dt} = \int_\Sigma \frac{\partial d_1}{\partial t} d\Sigma' + \oint_\zeta (d_1\mu)d\lambda, \quad (3.2)$$

where the second integral is over $\zeta$, the perimeter of $\Sigma$, and $\mu$ defines the velocity of the curve $\zeta$ normal to itself (such that positive values of $\mu$ increase $\Sigma$). The coordinates $\lambda$ and $n$ form a right-handed coordinate system, with $\lambda$ directed along $\zeta$, and $n$ directed out of $\Sigma$ (or into negative $\Sigma$). Thus, $\mu$ is given by

$$\mu = \alpha \frac{q_t}{q_n}, \quad (3.3)$$

where $\alpha$ is $-1$ on that part of $\zeta$ consisting of $q_1 = q_0$, and 0 on that part of $\zeta$ consisting of $\theta = \theta_0$, and the subscripts $t$ and $n$ denote differentiation with respect to time and $n$, respectively.

To evaluate the first integral on the rhs of (3.2), consider the potential vorticity balances in the two layers. If we assume the length scales of the problem to be large enough so that relative vorticity (and friction) may be ignored, then the potential vorticity equations for the two layers are well approximated by

$$\frac{\partial d_1}{\partial t} + \frac{1}{\rho_0} J\left(P_1, \frac{d_1}{f}\right) = w_{\text{Ek}}, \quad (3.4)$$

$$\frac{\partial d_2}{\partial t} + \frac{1}{\rho_0} J\left(P_2, \frac{d_2}{f}\right) = 0, \quad (3.5)$$

where $P_1$ and $P_2$ are the upper- and lower-layer perturbation pressure fields. Note that (3.5) is the topographic Sverdrup balance, with $\partial d_2/\partial t$ $(= -\partial d_1/\partial t)$ acting as a surrogate pumping velocity. Regardless of the length scales imposed on the problem, this balance would not generally be possible were it not for the blocked nature of the abyssal potential vorticity field. Similarly, (3.4) is equivalent to a Sverdrup balance in which the Ekman pumping velocity is given by $w_{\text{Ek}} - \partial d_1/\partial t$. Since potential vorticity contours in the upper layer are not blocked, this balance cannot be expected to persist unless $\partial d_1/\partial t = w_{\text{Ek}}$, so that the effective pumping velocity is zero. Taking this to be the case, the first integral on the rhs of (3.2) reduces to

$$\int_\Sigma \frac{\partial d_1}{\partial t} d\Sigma' \approx \int_\Sigma w_{\text{Ek}} d\Sigma'. \quad (3.6)$$

The time derivative of $V$ must also be equal to the sum of the fluxes across $\zeta$. If we ignore ageostrophic fluxes other than the Ekman flux, then

$$\frac{dV}{dt} = \oint_\zeta (\mathbf{V}_g + \mathbf{V}_e)\cdot \mathbf{n} d\lambda, \quad (3.7)$$

where $\mathbf{V}_g$ and $\mathbf{V}_e$ are geostrophic and Ekman fluxes into $\Sigma$. That is, $\mathbf{V}_g$ and $\mathbf{V}_e$ are both measured relative to the velocity of the curve $\zeta$ itself, that is,

$$\mathbf{V}_g \cdot \mathbf{n} = d_1(\mathbf{v}_g \cdot \mathbf{n} - \mu) \quad (3.8a)$$

and

$$\mathbf{V}_e \cdot \mathbf{n} = d_e(\mathbf{v}_e \cdot \mathbf{n} - \mu), \quad (3.8b)$$

where $\mathbf{v}_g$ and $\mathbf{v}_e$ are the geostrophic and Ekman velocity fields, with the latter being an average taken over the

Ekman layer depth, $d_e$. If $d_e$ is taken to be negligibly thin, then, using (3.6), the first integral on the rhs of (3.2) is approximately equal to the net contribution of the Ekman fluxes in (3.7). Equating the two expressions for $dV/dt$, we thus have

$$\oint_{\zeta} (\mathbf{V}_g)\cdot \mathbf{n}\, d\lambda \approx \oint_{\zeta} (d_1\mu) d\lambda. \qquad (3.8c)$$

Using (3.1), it is then possible to show that the geostrophic flux across $\theta = \theta_0$ must be zero:

$$\oint_{\theta=\theta_0} (\mathbf{V}_g)\cdot \mathbf{n}\, d\lambda$$

$$= \oint_{\zeta} (\mathbf{V}_g)\cdot \mathbf{n}\, d\lambda - \oint_{q_1=q_0} d(\mathbf{v}_g\cdot \mathbf{n} - \mu) d\lambda$$

$$= \oint_{\zeta} (d\mu) d\lambda - \oint_{q_1=q_0} (d\mu) d\lambda = 0. \qquad (3.9)$$

Thus, during spinup (typically the first several years of integration), there can be little upper-layer geostrophic flux across those latitude circles that intersect zonally reconnecting potential vorticity contours. Equivalently, over this latitude band, there is essentially no vertical transmission of angular momentum via interfacial form stresses. Assuming this latitude band to be fairly extensive, then the overall angular momentum balance during the spinup phase can be summarized as follows: The wind-stress torque drives an equatorward Ekman flux, increasing the total moment of inertia of the upper layer. In the lower layer, pressure torques, nearly equal and opposite to the wind-stress torque, effect a net poleward transport of mass. This decreases the moment of inertia (i.e., the planetary angular momentum) in that layer. The small difference between these two large torques results in a small acceleration of the zonal current in the upper layer.

The upper layer, during this spinup phase, behaves much as would be expected of a 1½-layer model. That is, because circumpolar flow is prohibited in the lower layer, the tilting of the interface height field must serve primarily to counterbalance the upper-layer pressure gradients. The zonal current, therefore, accelerates roughly in proportion to the meridional gradient of the Ekman pumping field. The potential vorticity balance of the lower layer is essentially a Sverdrup balance, with the continual tilting of the interface between the two layers serving as the pumping velocity.

These results depend on the existence of blocked geostrophic contours in the lower layer (otherwise relative vorticity could not have been neglected). Relative vorticity will also become important once smaller-scale eddies are introduced into the problem. This can be expected to happen once the flow becomes baroclinically unstable. Since there must be a vertical transfer of angular momentum in the statistically steady state, it is therefore likely that the statistically steady state will be baroclinically unstable.

## 4. An estimate of transport

The need for transient eddies in the statistically steady state can also be inferred directly from the requirement that the meridional circulation must be closed in each of the layers individually. Let $\Gamma$ be the region lying north of the zonally reconnecting $q_1$ contour $q_1 = q_0$. On average, the flux of upper-layer water out of this region must be zero. If $Q$ is the average Ekman transport across this curve, then, assuming ageostrophic fluxes in the interior to be small, the average geostrophic transport out of $\Gamma$ must be equal and opposite to $Q$. That is,

$$\oint_{q_1=q_0} d\left(\mathbf{v}_g\cdot \mathbf{n} + \frac{q_t}{q_n}\right) d\lambda = -Q. \qquad (4.1)$$

If there is no time dependence in the problem, then (3.1) implies that (4.1) is an impossibility unless $Q = 0$. If $Q$ differs from zero, then the required geostrophic flux out of $\Gamma$ must be accomplished by the second term on the lhs of (4.1). Put another way, transient eddies are needed to close the meridional circulation in the upper layer. If we assume that these eddies result from baroclinic instability of the mean flow, then the necessary condition for baroclinic instability may be considered a prerequisite to the statistical steady state.

The arguments used here to conclude that the transport should be confined primarily to the upper layer were based on the existence of blocked geostrophic contours in the lower layer. The existence of these contours is related to the fact that topography crosses the channel, so that isobaths intersect the vertical walls of

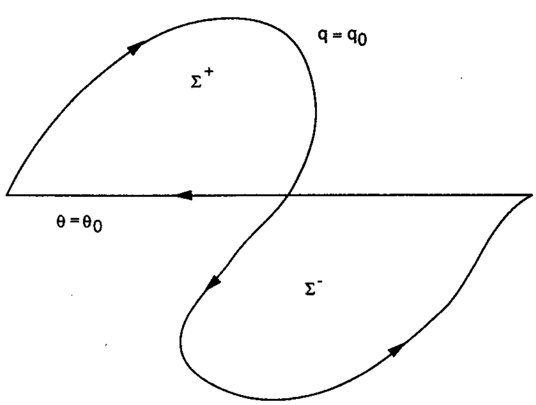


FIG. 1. Here $\Sigma$ is defined as the area bounded by $\zeta$, the union of the curves $q = q_0$ and $\theta = \theta_0$. Area south of $\theta = \theta_0$ is considered negative. The coordinates $\lambda$ and $n$ form a right-handed system, with $n$ normal to $\zeta$ and pointing out of (positive) $\Sigma$. Arrows denote the direction of increasing $\lambda$.

the channel. In the real ocean, there are, of course, no vertical walls, and in this sense, isobaths that "block" the channel cannot be found. In general, however, one expects the abyssal layers to intersect ocean topography, so that circumpolar flow is not possible in these layers. It is also probable that, slightly higher up in the water column the dynamics correspond more closely to the dynamics of blocked geostrophic contour regimes (e.g., Sverdrup gyres). In this sense, we believe the assumption of a limited circumpolar flow at depth to be fairly robust.

Given that the zonal current is confined to the upper layer, we can use the necessary condition for baroclinic instability to derive an estimate for the transport around the channel. The former states that for baroclinic instability to occur, there must be a reversal in the gradient of $q$ with depth. This occurs when

$$\eta_\theta > d_2 \cot\theta, \qquad (4.2)$$

that is, when the meridional variations in $q_2$ due to stretching effects become larger than those due to the planetary $\beta$ effect. Using the thermal wind relation and the fact that the flow is essentially confined to the upper layer, (4.2) can be rewritten as

$$u_1 > \frac{g'\beta d_2}{f^2}. \qquad (4.3)$$

Furthermore, since $u_1 \gg u_2$, the barotropic velocity $u_b$ may be written as $u_b \approx d_1 u_1 / d_T$, where $d_T \equiv d_1 + d_2$, so that (4.2) becomes

$$u_b > \frac{g'\beta d_1 d_2}{f^2 d_T} = c_R, \qquad (4.4)$$

where $c_R$ is the baroclinic long–Rossby wave speed. Thus, the necessary condition for baroclinic instability is met once the flow becomes supercritical with respect to the long–Rossby wave speed. Although the necessary condition for baroclinic instability only requires that $u_b$ be greater than $c_R$ somewhere in the channel, we will assume the flow to be baroclinically unstable over a substantial portion of the channel. The Rossby wave speed can then be used as a rough estimate for an average value of $u_b$. This leads to an estimate of transport at the time instabilities first occur:

$$\text{transport} \approx \beta d_T (l_\rho)^2 L_y, \qquad (4.5)$$

where $L_y$ is the meridional extent of the channel and $l_\rho$ is the baroclinic Rossby radius ($l_\rho^2 = g' d_1 d_2 / f^2 d_T$) evaluated, say, in the center of the channel. An interesting aspect of (4.5) is that it predicts a transport, independent of the wind stress (although it is assumed that the wind stress is sufficiently strong so that there is a nontrivial Ekman transport across a typical closed $q_1$ contour).

Some caution must be used when comparing the transport predicted by (4.5) to numerical experiments in the literature (e.g., TM; WMRO). Recall that (4.5) assumes there to be little or no circumpolar transport in the abyssal layer. Thus, for example, numerical runs using topography in the form of a Gaussian bump (isolated from the channel walls) can be expected to have a considerable band of zonally reconnecting $q$ contours (and hence transport) in the abyssal layer. In such cases, (4.5) applies to the thermal wind transport only (e.g., the transport calculated by assuming the lower layer to be at rest and using thermal wind to get the upper-layer transport). In addition, experiments for which there are large latitude bands near the center of the channel over which the bottom is flat tend to develop exceedingly large barotropic currents. The horizontal shear in these currents then tends to inhibit the growth of baroclinically unstable mode (James 1987). In cases such as these, therefore, the necessary condition for baroclinic instability is typically not sufficient, and (4.5) underestimates even that part of the transport associated with the thermal wind.

Equation (4.5) might also be considered an underestimate in that, for a stronger wind stress, one expects that a more vigorous eddy field will be necessary to close the meridional circulation. Presumably, a stronger eddy field would require a stronger reversal in the reversal of $\nabla q$ with depth. It is interesting to note that an increase in the strength of the $\nabla q$ reversal need not imply a large increase in transport. That is, the tilt in the interface height field necessary to achieve a weak reversal in the gradient of $q$ is large with respect to that required to, say, double the strength of the reversal (e.g., as measured by $\nabla q_2 / \nabla q_1$). Thus, independently of the strength of the winds, we expect that an eddy field, sufficiently strong so as to enable the upper-layer meridional circulation to reach a steady state, should develop soon after the necessary condition for baroclinic instability is reached. (An exception to this is mentioned in the preceding paragraph).

In cases for which the barotropic current is not exceedingly strong, however, (4.5) can be compared to (numerical) observations. Table 1 makes this comparison with several of the numerical runs discussed

TABLE 1. Comparison of transport predicted by (4.5) with various numerical experiments from WMRO. Agreement between our estimate and the thermal wind portion of their reported transports is quite good. [The thermal wind transports were calculated at $T_1 - D_1/D_2\,(T_2)$, where $D_1$ and $D_2$ are the upper- and lower-layer mean depths (1000 m and 4000 m, respectively) and $T_1$ and $T_2$ are the upper- and lower-layer transports]. All transports are in Sverdrups.

| | Layer | | | | |
|---|---|---|---|---|---|
| | Upper | Lower | Both | Thermal wind | Our estimate |
| M1 | 132 | 112 | 244 | 104 | 88 |
| M2 | 73 | −26 | 47 | 79.5 | 88 |
| BR | 84 | −14 | 70 | 80.5 | 88 |

by WMRO (cf. their Table 3). In particular, we consider their cases D1, D2, and BR. Cases D1 and D2 have topography in the form of two partially blocking ridges, one stemming from the northern boundary and the other from the southern boundary. In D1, each of these extend roughly one-third of the way across the channel (at different longitudes). Case D2 is similar, except that each ridge extends two-thirds of the way across the channel. Case BR has topography in the form of a single ridge that spans the width of the channel (see their Fig. 8). In all three cases the following parameters apply: $d_1 \approx 1000$ m, $d_2 \approx 4000$ m, $L_W = 1500$ km, $l_\rho = 32$ km, and $\beta \approx 1.15 \times 10^{-11}$ m$^{-1}$ s$^{-1}$. (This value for $\beta$ is inferred from their choice of $f_0$ of $-1.263 \times 10^{-4}$ s$^{-1}$.) Agreement between (4.5) and the "thermal wind" portion of the transport is good in all three cases. Although the $q_2$ fields are not shown in WMRO, it seems probable from the topographies that cases D2 and BR have at best a narrow band of zonally reconnecting $q_2$ contours. Thus, a large circumpolar flow in the abyssal layer would be unlikely in these two experiments. In fact, the reported lower-layer transports are slightly westward so that the total transport is less than predicted by (4.5). In case D1, by contrast, it is likely that there is a considerable band of zonally reconnecting $q_2$ contours so that a substantial flow in the lower layer is possible, and one expects (4.5) to underestimate the total transport. Indeed, the reported lower-layer transport for this case is positive (and of the same order of magnitude as the upper-layer transport). In this instance, therefore, it would seem that the existence of pathways allowing for free circumpolar flow in the lower layer have effectively tripled the (total) transport.

In the Southern Ocean, the baroclinic Rossby radius is typically less than the 32 km used in the previous example (e.g., WMRO; Houry et al. 1987). In addition, the width of Drake passage is about one-half the value used for $L_W$.[1] If, for example, we take $l_\rho$ and $L_w$ to be 2/3 and 1/2, respectively, of their values in the previous example, then (4.5) predicts a reduction of transport by a factor of 2/9. That is, the predicted transport is on the order of 20 Sv. When this estimate is combined with Baker's (1982) estimate for the contribution to the total transport associated with interactions between the ACC and the subpolar gyre, an estimate of 189 $\pm \sim 100$ Sv for the total transport through Drake Passage is obtained. (Baker's estimate is based on the net Sverdrup–Ekman transport across 55°S, excluding a small region between 70°W and 40°W just east of Drake Passage.) The precision of this estimate is poor. Additional uncertainty in Baker's estimate arises from his assumption of a linear Sverdrup balance. Given the observed eddy field, for example, it is likely that the dynamics will more closely obey a turbulent Sverdrup balance. Nevertheless, the estimate is in general agreement with reported observed values ($\sim$130 Sv, Whitworth et al. 1982) and with values obtained by more realistic numerical models (e.g., $\sim$190 Sv, The FRAM Group 1991).

While the idea of gyrelike dynamics setting the transport of the ACC is not new, it has long been considered inadequate because these dynamics have been difficult to apply at Drake Passage latitudes. The preceding arguments, however, suggest that the additional dynamics necessary where there are zonally reconnecting geostrophic contours need not imply a large additional transport.

[1] It is not clear, however, whether the width of Drake Passage (as suggested in the text) is the most appropriate choice of our parameter $L_w$. It could be, for example, that a "typical" width of the band of zonally reconnecting contours would be more appropriate. This need not coincide with the width of Drake Passage.

*Acknowledgments.* The bulk of this work was carried out as part of the author's Ph.D. thesis at the University of Washington under the direction of Peter Rhines. Sincere thanks are expressed to him for his help and encouragement. Comments from two anonymous reviewers helped to shorten and clarify the original manuscript. One reviewer also made helpful comments regarding the role of transient eddies. While at the University of Washington, the author was supported by NSF Grant OCE 86-13725.

## REFERENCES

Baker, D. James, 1982: A note on the Sverdrup balance in the Southern Ocean. *J. Mar. Res.*, **40**(Suppl.), 21–26.

FRAM Group, 1991: An eddy-resolving model of the Southern Ocean. *Eos, Trans., Amer. Geophys. Union,* **72**, 169–175.

Houry, S., E. Dombrowsky, P. De Mey, and J.-F. Minster, 1987: Brunt–Väisälä frequency and Rossby radii in the South Atlantic. *J. Phys. Oceanogr.*, **17**, 1619–1626.

James, I. N., 1987: Suppression of baroclinic instability in horizontally sheared flows. *J. Atmos. Sci.*, **44**, 3710–3720.

McWilliams, J. C., W. R. Holland, and J. H. S. Chow, 1978: A description of numerical Antarctic Circumpolar Currents. *Dyn. Atmos. Oceans,* **2**, 213–291.

Munk, W. H., and E. Palmén, 1951: Note on the dynamics of the Antarctic Circumpolar Current. *Tellus,* **3**, 53–55.

Stommel, H., 1957: A survey of ocean current theory. *Deep-Sea Res.*, **4**, 149–184.

Treguier, A. M., and J. C. McWilliams, 1990: Topographic influences on wind-driven, stratified flow in a $\beta$-plane channel: An idealized model for the Antarctic Circumpolar Current. *J. Phys. Oceanogr.*, **20**, 321–343.

Whitworth, T., III, W. D. Nowlin, Jr., and S. Worley, 1982: The net transport of the Antarctic Circumpolar Current through Drake Passage. *J. Phys. Oceanogr.*, **12**, 960–971.

Wolff, J.-O., E. Maier-Reimer, and D. J. Olbers, 1991: Wind-driven flow over topography in a zonal $\beta$-plane channel: A quasigeostrophic model of the Antarctic Circumpolar Current. *J. Phys. Oceanogr.*, **21**, 236–264.